

Research Article

# Comparison of Graphene Oxide-Titanium Oxide (GO-TiO<sub>2</sub>) Composite Film Coating Methods on Glass Substrates and Surface Characterization Study

İbrahim Fırat Balkaya<sup>1\*</sup>, Harun Mindivan<sup>2</sup> and Nevin Atalay Gengec<sup>3</sup>

<sup>1</sup>Bilecik Seyh Edebali University, Institute of Graduate, Mechanical Engineering Department, 11210, Gulumbe, Bilecik, Turkey. (e-mail: 1055242@ogrenci.bilecik.edu.tr).

<sup>2</sup>Bilecik Seyh Edebali University, Mechanical Engineering Department, 11210, Gulumbe, Bilecik, Turkey. (e-mail: harun.mindivan@bilecik.edu.tr).

<sup>3</sup>Kocaeli University, Department of Environmental Protection Technologies, 41001, Izmit, Kocaeli, Turkey. (e-mail:nevin.atalay@kocaeli.edu.tr).

## ARTICLE INFO

Received: Aug., 20. 2024

Revised: Sep., 08. 2024

Accepted: Sep., 09. 2024

### Keywords:

Graphene oxide

Titanium oxide

Dip coating

Spin coating

Contact angle

Corresponding author: *İbrahim Fırat BALKAYA*

ISSN: 2536-5010 | e-ISSN: 2536-5134

DOI: <https://doi.org/10.36222/ejt.1536083>

## ABSTRACT

In this work, graphene oxide-titanium oxide (GO-TiO<sub>2</sub>) nanocomposite was successfully produced via ultrasonication process. For coating process, spin coating (SC), dip coating (DC) and spray coating methods were used. The synthesized nanocomposite and surfaces were characterized by optical microscope, SEM, EDX, FTIR, XRD, four-probe conductivity, water contact angle.

As result of experiments, while spin coating provides thinner coating, a thicker and higher water contact angle surface was formed under the optimum condition of dip coating. XRD, four-probe conductivity results revealed partial formation of reduced graphene oxide within the composite structure. Water contact angle results showed that the best result regarding stability of droplet shape was on the spin coated surface. On the other hand, it was observed that deionized water test liquid droplet on the dip coated surfaces stabilized relatively slower but provided a much higher water contact angle.

## 1. INTRODUCTION

Graphene oxide (GO) thin films are typically synthesized from graphite using the Hummers method [1]. These thin films are generally applied to surfaces using techniques such as spin coating, dip coating, or spray coating. In the literature, there are applications for increasing some properties by creating various metal oxide-GO and hydrocarbon-GO composites [2,3]. Titanium dioxide (TiO<sub>2</sub>) thin films, on the other hand, can be prepared using methods like sol-gel, Chemical Vapor Deposition (CVD), or Atomic Layer Deposition (ALD) [4]. Composite thin films formed by combining these two materials bring together the advantages of both GO and TiO<sub>2</sub> [5].

In addition to thermodynamic-based solutions in energy storage and transmission, niche studies on metals and phase change materials continue to increase [6, 7]. Graphene and graphene oxide-based solutions are also widely used in electrical-based studies for similar purposes. GO and TiO<sub>2</sub> hold significant positions in the fields of nanotechnology and materials science. GO is notable for its large surface area, excellent conductivity, and surface functionalization

capabilities, while TiO<sub>2</sub> is known for its superior photocatalytic activity and chemical stability [8, 9]. When GO's high surface area, excellent electrical conductivity, and mechanical durability are combined with TiO<sub>2</sub>'s high photocatalytic activity and chemical stability, multifunctional thin films can be produced. Coating these materials as thin films has great potential, particularly in fields such as energy storage, environmental cleaning, and biomedical applications [10]. GO-TiO<sub>2</sub> thin films are especially important for applications in dye-sensitized solar cells, supercapacitors, and wearable electronic devices [11]. The high photocatalytic activity of TiO<sub>2</sub> under UV light can be broadened to a wider spectrum when supported by GO, thereby increasing photocatalytic efficiency [5]. Moreover, the antibacterial properties of these materials allow them to be used as surface coatings in biomedical devices [12].

The preparation of stable GO-TiO<sub>2</sub> dispersions is crucial for ensuring the homogeneous distribution and long-term stability of these materials. Various methods are found in the literature. One such method is the addition of various surfactants to enhance dispersion stability. These surfactants reduce interactions between particles, preventing

agglomeration and thereby making the dispersion more stable [13]. Ultrasonication is a commonly used method for achieving homogeneous mixing of GO and TiO<sub>2</sub> and obtaining a stable dispersion. Ultrasonication methods provide significant control over the structure, size, and distribution of nanoparticle components [14]. The use of high-speed mixing following sonication is an effective method for achieving homogeneous distribution of GO and TiO<sub>2</sub> particles [15]. The obtained GO-TiO<sub>2</sub> dispersions have demonstrated long-term stability and homogeneous distribution. As reported in the literature, the use of ultrasonic methods minimizes the risk of aggregation by ensuring the homogeneous distribution of particles, while the presence of oxygen-related functional groups, such as -OH and -COOH, in GO serves as ideal support for carrying TiO<sub>2</sub> nanocrystals [16]. This method facilitates more efficient results in photocatalytic applications.

For coating a stable dispersion onto a suitable substrate, methods such as spin coating [17], dip coating, and spray coating [18] are commonly used.

This study aims to successfully deposit GO-TiO<sub>2</sub> composite films on glass substrates and to compare the effects of different coating methods on the surface properties of GO-TiO<sub>2</sub> composite films.

## 2. Materials and Methods

In this study, a dispersion was prepared using the ultrasonication method. The obtained dispersion was used to create coatings/surfaces on 25x75mm glass substrates via dip coating, spin coating, and spray coating methods. X-ray Diffraction (XRD) (Panalytical/Empyrean) and Fourier-Transform Infrared spectroscopy (FTIR) (Perkin Elmer/Spectrum100) analyses of GO and GO-TiO<sub>2</sub> composites were conducted, and their conductivity was compared using a four-probe conductivity device (Signatone). To assess the homogeneity of the surface and hydrophobic properties, the equilibrium contact angle ( $\theta_e$ , °) of water (deionized water-Merck) was evaluated using an optical contact angle measurement device (Biolin Scientific/Theta Lite). The test liquid droplet volume was set at 4 $\mu$ L. Other characterization methods used in this study include optical microscopy (Nikon Eclipse/LV150), Scanning electron microscope (SEM) (Zeiss/SupraV40), and Scanning Electron Microscopy with Energy Dispersive X-ray spectroscopy (SEM-EDX) (Bruker).

## 3. EXPERIMENTS

### 3.1. Preparation of Stable GO-TiO<sub>2</sub> Dispersion

The preparation of stable dispersions generally involves steps of ultrasonication, mixing, and centrifugation [19]. A mixture of graphene oxide with an initial concentration of 2 mg/mL was obtained by adding 1g of graphite oxide (GrO) into 500 mL of deionized water (Merck). This mixture was subjected to ultrasound at 35 kHz for 16 hours and then centrifuged at 3000 rpm for 30 minutes. The supernatant obtained after centrifugation is the stable GO dispersion, and its concentration was found to be 0.83 mg/mL according to the solid content analysis. The stable GO-TiO<sub>2</sub> dispersions were prepared using a new formulation with TiO<sub>2</sub>, similar to the GO/SnO<sub>2</sub> stable dispersions prepared by Liang et al. [20] using SnO<sub>2</sub>, as described below. The stable GO dispersion was diluted with deionized water (Merck) water to a concentration

of 0.8 mg/mL and subjected to ultrasonication for 5 minutes. Then, 0.1 g of TiO<sub>2</sub> was added to 250 mL of the stable GO dispersion and ultrasonicated for 1.5 hours. The prepared dispersion was centrifuged at 3000 rpm for 5 minutes, and the supernatant was collected. The concentration of the GO/TiO<sub>2</sub> dispersion after centrifugation was found to be 0.6 mg/mL based on solid content analysis. The obtained GO-TiO<sub>2</sub> dispersion remained stable for two weeks and was used in the production of GO-TiO<sub>2</sub> surfaces. It has been reported that the strong interactions of TiO<sub>2</sub> nanocrystals with GO layers prevent their detachment during the ultrasonication process [21].

### 3.2. GO-TiO<sub>2</sub> Coating Studies

The first step of the coating process involves imparting properties to the glass substrate that allow it to retain the coating. For this purpose, the glass substrates were cleaned with deionized water after a 30-minute chromic acid bath and dried in a vacuum oven, followed by 5s of vacuum plasma treatment.

In this study, surfaces were obtained by coating glass substrates using dip coating, spin coating and spray coating methods. Since the spin coating method involves too many parameters and the variation in experimental parameters and results is very complex, it was carried out under optimum experimental conditions determined by discussing in detail in another study. The spin coating (Figure 1.a) parameters were set as a spinning speed of 500 rpm (SC500), a spinning time of 10s, and a coating fluid volume of 0.3 mL. Dip coating was performed (Figure 1.b) at four different speeds: 240 (DC240), 320 (DC320), 400 (DC400), and 480 (DC480) mm/min for both immersion and withdrawal. Spray coating (Figure 1.c) was applied to the glass substrate material, heated to approximately 300°C, differing from the other two experiments.

The images of the surfaces produced by spin coating and dip coating methods are shown in Figures 2.a and 2.b, respectively.

## 4. RESULTS and DISCUSSION

According to the obtained FTIR results (Figure 3), the peak at 1627 cm<sup>-1</sup> originates from non-oxidized C=C bonds, while the peaks in the "2800-3000 cm<sup>-1</sup>" region are due to -OH stretching vibrations. The peaks between "2000-2250 cm<sup>-1</sup>" indicate the presence of reduced graphene oxide (rGO) [22]. The region between "1750-1040 cm<sup>-1</sup>" corresponds to carboxyl groups, with the peak at 1708 cm<sup>-1</sup> attributed to C=O, the peak at 1430 cm<sup>-1</sup> to C-O, and the peak at 1375 cm<sup>-1</sup> to C-O-C (epoxy) or C-O-H (phenolic) structures. The peak at 1154 cm<sup>-1</sup> identifies alkoxy C-O carboxyl. In the GO-TiO<sub>2</sub> composite, it was observed that the peaks corresponding to oxygen functional groups seen in GO disappeared, and peaks related to Ti-O-Ti and Ti-O-C stresses emerged in the "500-900 cm<sup>-1</sup>" range [23]. The XRD analysis of the GO-TiO<sub>2</sub> composite (Figure 4) shows a characteristic peak of GO at approximately 2 $\theta$ ≈11° and a peak specific to titanium at approximately 2 $\theta$ ≈26° [24, 25].

Conductivity measurements using a four-point probe are consistent with partial graphene formation. The surface exposed to the oven atmosphere in GO solid and GO-TiO<sub>2</sub> solid generally exhibits low conductivity. When comparing the two materials, it was concluded that the conductivity in

GO-TiO<sub>2</sub> solid/precipitate is much higher than in GO solid/precipitate (Tables I and II).

This result indicates that a reduced graphene oxide-titanium oxide (rGO-TiO<sub>2</sub>) composite begins to form through

simple ultrasonication, as the peak at 2θ≈26° in the XRD results aligns with rGO-TiO<sub>2</sub> formation [26].

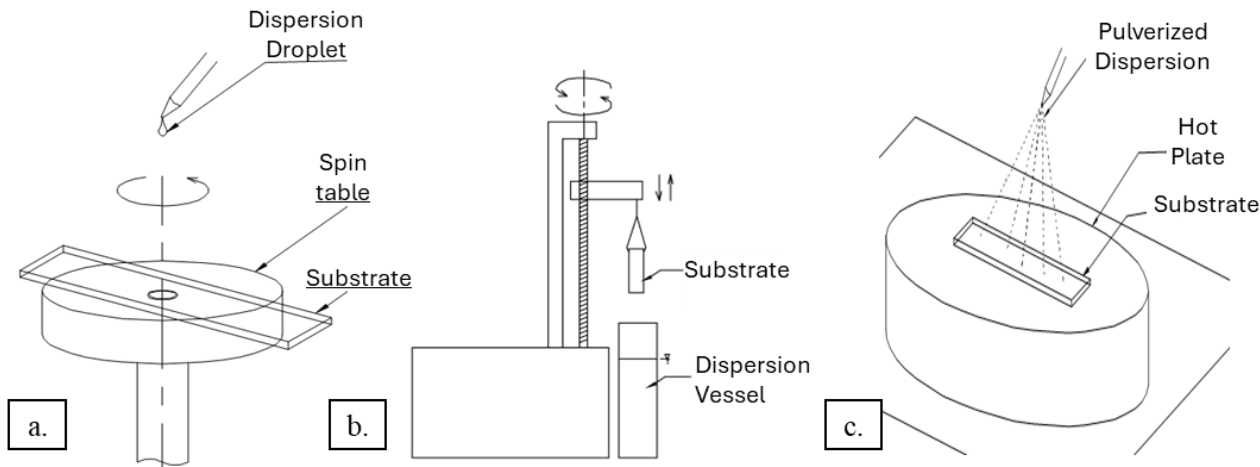


Figure 1. a. Schematic representation of dip coating, b. spin coating, c. spray coating on heated substrate.



Figure 2. Images of surfaces produced on glass slide substrates by a. spin coating method and b. dip coating method.

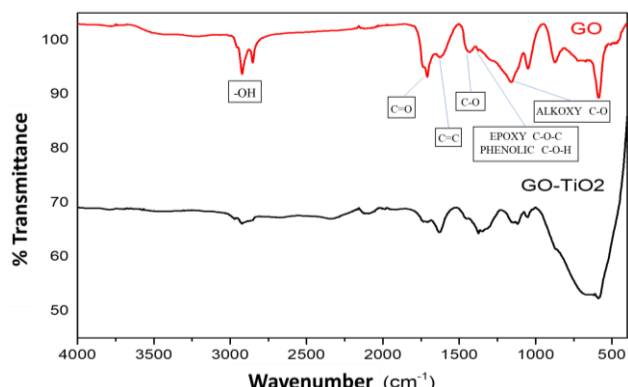


Figure 3. FTIR spectrum of GO and GO-TiO<sub>2</sub>.

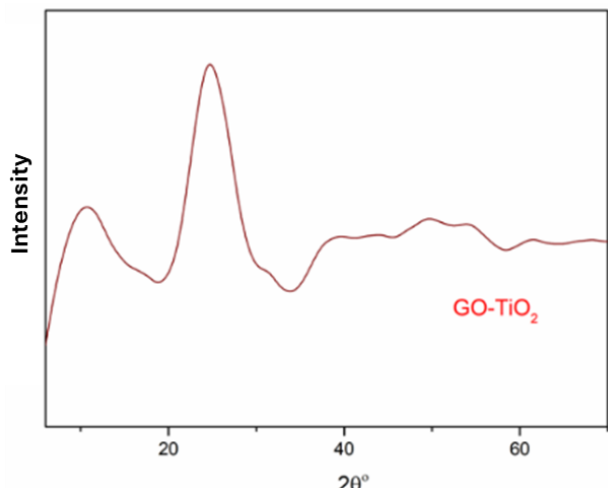


Figure 4. XRD analysis of the GO-TiO<sub>2</sub> composite

TABLE I

CONDUCTIVITY MEASUREMENTS OF THE SOLID CONTENT/PRECIPIRATE OF GO-DEIONIZED WATER SUPERNATANT.

Current (mA)	Thickness (µm)		V/I	Specific Cond. σ	S/m	S
	Rs (ohm/sq)	Res (ohm-cm)				
0,005	1	1				
Point						
1	15996,3350	1,5996	4034,8403	0,62514	0,006251	0,000248
2	22661,5527	2,2662	4965,2769	0,44128	0,004413	0,000201

TABLE II

CONDUCTIVITY MEASUREMENTS OF THE SOLID CONTENT/PRECIPIRATE OF GO-TiO<sub>2</sub>-DEIONIZED WATER SUPERNATANT.

Current (mA)	Thickness (µm)		V/I	Specific Cond. σ	S/m	S
	Rs (ohm/sq)	Res (ohm-cm)				
0,005	1	1				
Point						
1	4831,685547	0,483169	1302,066284	2,06967	0,020697	0,000768
2	4300,179199	0,430018	859,313416	2,32548	0,023255	0,001164

Table III presents the results of dip coating experiments conducted at four different speeds of 240, 320, 400, and 480 mm/min, respectively, for both immersion and withdrawal. According to the water equilibrium contact angle measurements, the contact angle values decreased as the dipping speed increased in dip coating process. Additionally, the time-dependent stability of the droplet profile, which is an indication of the homogeneity of the coating, was investigated. The most consistent time-dependent angular change curve was obtained in the dip coating experiment conducted at 320 mm/min, and the contact angle became asymptotic to the time axis within 2s. Although the coating produced at 240 mm/min exhibited a consistent change curve compared to the contact angle-time curves of 400 mm/min and 480 mm/min, it did not become asymptotic to the time axis even after 3s of

measurement. Despite extending the test duration to 6s due to the continuous decrease in the contact angle-time curves of DC400 and DC480, the angle value kept decreasing and never became asymptotic.

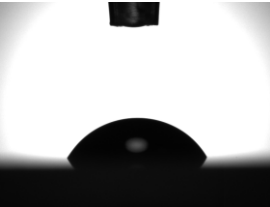
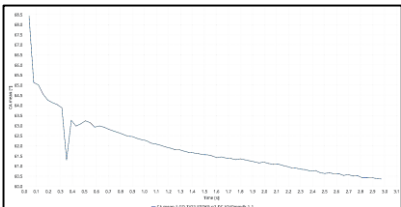

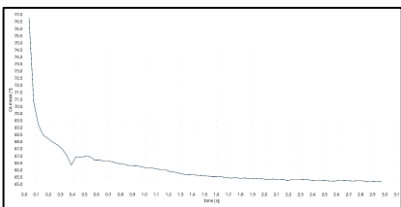

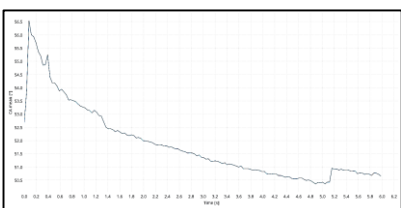

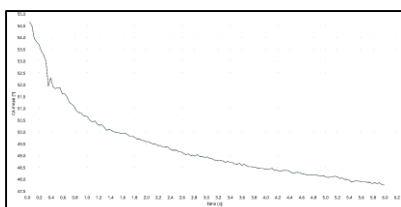
In the DC320 GO-TiO<sub>2</sub> thin film coating (Figure 5), the "surface" formation is seen in optical microscope images as Ti-rich (light-colored) regions with TiO<sub>2</sub> particles (dark-colored spots) within them. The surface appearance obtained by the spin coating method is essentially the same, but it has a thinner, more homogeneous, and densely distributed structure (Figure 7). SEM images of the obtained DC320 GO-TiO<sub>2</sub> thin film coatings could only be taken after double platinum coating due to their low conductivity (Figures 6 and 8a). TiO<sub>2</sub> particles appear as light-colored in the surfaces obtained by both methods. The presence of light-colored TiO<sub>2</sub> particles in the SEM images is consistent with the literature [27].

In the spin coating study, the optimal values determined were a spinning speed of 500 rpm for 10s and the use of 0.3 mL of stable dispersion, yielding a contact angle of approximately 58.5°. It was observed that the change in the contact angle rapidly became parallel to the time axis (Table IV).

When the spin coating and dip coating methods were compared in terms of TiO<sub>2</sub> particle adhesion and distribution on the surface, it was observed that the spin coating method resulted in a significantly higher adhesion amount and a more regular distribution (Figures 5 and 7). Elemental EDX results reveal the presence of Si and other elements originating from the sodium glass substrate in addition to Ti.

The spray coating experiment was conducted on a glass substrate heated to 300°C. Due to the nature of the process, the presence of droplets that rapidly dry on this surface results in a structure composed of peaks and pits, which is clearly observed in the SEM images (Figure 9.a and b). Another expected outcome of the spray coating process is that GO-TiO<sub>2</sub> undergoes some degree of thermal reduction, leading to the formation of a rGO-TiO<sub>2</sub>. Due to the non-uniformity of the surface roughness and the extreme roughness compared to the other two surfaces, it was not possible to perform water contact angle measurements.

TABLE III  
CONTACT ANGLES AND THEIR TIME-DEPENDENT CHANGES FOR DIFFERENT DIPPING SPEEDS IN DIP COATING.

Sample	Contact Angle (θe, °)	Contact Angle Image	Time-dependent Contact Angle (θe°/s)
DC240	60,4		
DC320	65,5		
DC400	50,7		
DC480	47,7		

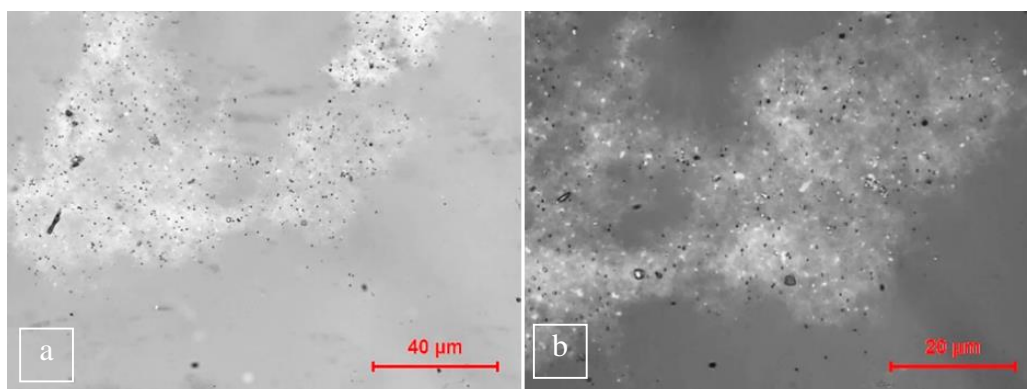


Figure 5. Optical microscope images of (DC320) GO-TiO<sub>2</sub> thin film coating obtained by the dipping method at a. X500 and b. X1000 magnification.

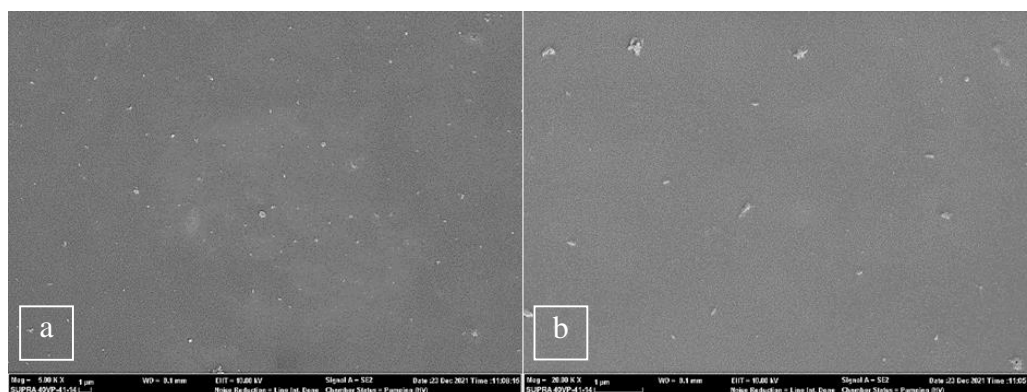
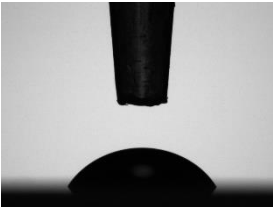
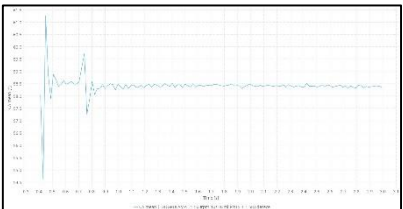


Figure 6. SEM images of (DC320) GO-TiO<sub>2</sub> thin film coating obtained by the dipping method at a. X5000 and b. X20000 magnification.

TABLE IV

CONTACT ANGLE AND ITS TIME-DEPENDENT CHANGE UNDER OPTIMAL CONDITIONS IN SPIN COATING.

Sample	Contact Angle (θe, °)	Contact Angle Image	Time-dependent Contact Angle (θe°/s)
SC500	58,5		

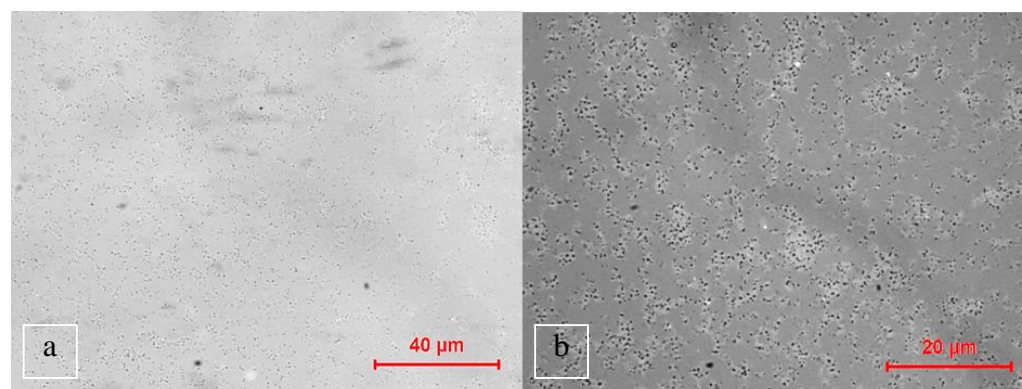
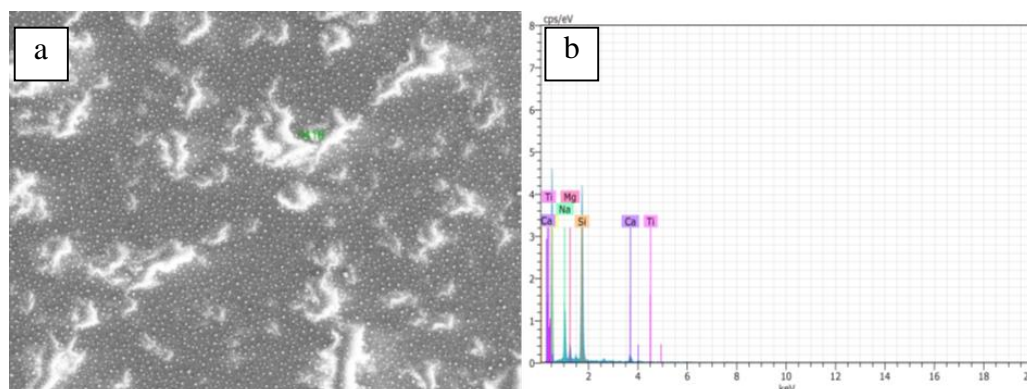
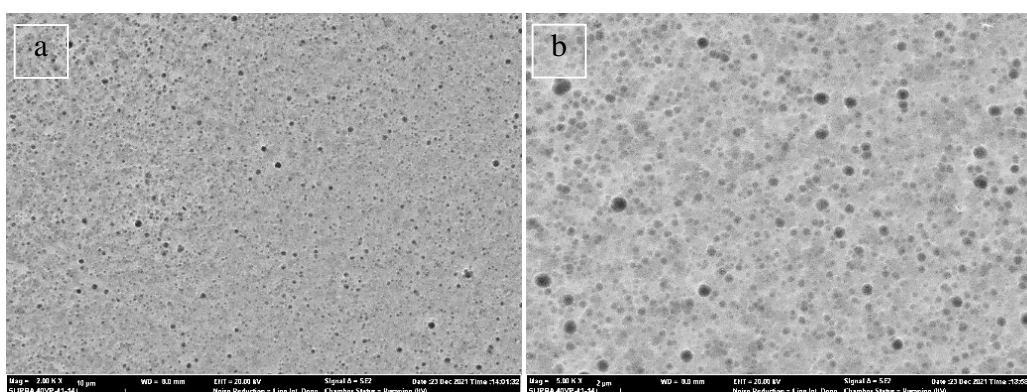


Figure 7. Optical microscope images of (SC500) GO-TiO<sub>2</sub> thin film coating obtained by the spin coating method at a. 500X and b. 1000X magnification.



**Figure 8. a.** SEM image at X2000 magnification and **b.** EDX results obtained at X2000 magnification of (SC500) GO-TiO<sub>2</sub> thin film coating produced by spin coating.



**Figure 9.** Scanning electron microscope (SEM) images of the GO-TiO<sub>2</sub> thin film coating obtained by the spray coating method at **a.** X2000 and **b.** X5000 magnification.

## 5. CONCLUSION

The aim of this study is to evaluate the effects of different coating techniques and parameters on the surface properties, particularly focusing on water contact angles and uniformity of GO-TiO<sub>2</sub> film coatings, and to highlight the importance of carefully selecting coating methods and parameters in order to tailor the surface properties and functionality of GO-TiO<sub>2</sub> films for specific industrial applications.

The most stable surface with the highest water contact angle (65°) using the dip coating was achieved at a speed of 320 mm/min. However, similar to the surface obtained in spin coating in this study, the contact angle values on non-substrate GO films generally range around 45° [28]. It is noted that GO exhibits hydrophilic properties due to the functionality of its oxygen-containing groups, such as -O-, -OH, and -COOH [29]. Bera et al. measured the contact angle of the GO coating on glass as 56°, and the contact angles obtained in the coating experiments are consistent with the literature [30]. The surfaces obtained by spray coating are irregular and chaotic due to the lack of control during the coating process. In spin coating, a thinner coating is observed, as seen in Figure 2. It is stated that an increase in the number of GO layers, that is, an increase in film thickness, leads to an increase in contact angle values [31]. When comparing spin coating to dip coating, it is observed that the water contact angle measurement droplet behaves more stably on the spin-coated surface. However, in the spin coating method, disruption of the integrity of the liquid film due to centrifugal force is evident from SEM and optical microscope images. According to Scidà et al. [32], variations in coating thickness significantly impact the conductivity of graphene-based film samples obtained by the reduction of graphene oxide

to graphene. Therefore, determining coating conditions, controlling coating thickness, and ensuring the homogeneous distribution of incorporated particles are of utmost importance.

In conclusion, the findings suggest that dip coating at controlled speeds could be optimized for applications requiring hydrophobic surfaces, while spin coating may be preferable for applications needing uniform conductivity and homogeneous surface properties of GO-TiO<sub>2</sub> coatings. Among the methods used, the dip coating method at a speed of 320 mm/min resulted in the most stable surface with the highest water contact angle. However, the spin coating method provided a more homogeneous coating, despite the occurrence of film tearing in micro scale due to centrifugal forces. The thickness of the coating, surface homogeneity, and particle distribution directly influenced the conductivity properties of the obtained films. It was emphasized that the coating method and conditions are crucial in determining these parameters.

## ACKNOWLEDGEMENT

This study was compiled from the results of the study carried out within the scope of project (Production of Graphene and Graphene-Based Slippery Liquid-Infused Porous Surfaces (Slips) Sensitive to External Stimuli and Determination of Their Smart Material Performance – Project No: 120M992BSEU – Project Group: 1001) supported by The Scientific and Technological Research Council of Turkey (TÜBİTAK). The researchers thank TÜBİTAK.

## REFERENCES

- [1] Hummers, W. S., & Offeman, R. E. (1958). Preparation of Graphitic Oxide. *Journal of the American Chemical Society*, 80(6), 1339.
- [2] Aydin, H. (2019). The effect of graphene oxide on the structural and electrical properties of yttrium ferrite based nanopowders. *European Journal of Technique (EJT)*, 9(1), 84-98.
- [3] Aydin, C. (2018). The Characterization of Morphology, Chemical and Optical Properties of Perylene Based Organic Nanocomposites Modified with Graphene Oxide. *European Journal of Technique (Ejt)*, 8(1), 99-109.
- [4] Chen, X., & Mao, S. S. (2007). Titanium dioxide nanomaterials: Synthesis, properties, modifications, and applications. *Chemical Reviews*, 107(7), 2891-2959.
- [5] Liu, X., Chen, C., Chen, X. A., Qian, G., Wang, J., Wang, C., ... & Liu, Q. (2018). WO<sub>3</sub> QDs enhanced photocatalytic and electrochemical performance of GO/TiO<sub>2</sub> composite. *Catalysis Today*, 315, 155-161.
- [6] Acir, A., Emin Canlı, M., Ata, I., & Erdi Tanürün, H. (2019). Effects of a circular-shaped turbulator having varying hole numbers on energy and exergy efficiencies of a solar air heater. *International Journal of Ambient Energy*, 40(7), 739-748.
- [7] Acir, A., Canlı, M. E., Ata, I., Uzun, S., & Tanürün, H. E. (2021). Experimental Investigation of Thermal Energy Storage Efficiency Using Fin Application with Phase Change Material (PCM) under solar radiation. *Heat Transfer Research*, 52(6).
- [8] Kamat, P. V. (2010). Graphene-based nanoarchitectures. Anchoring semiconductor and metal nanoparticles on a two-dimensional carbon support. *The Journal of Physical Chemistry Letters*, 1(2), 520-527.
- [9] Zhang, L., Liu, Q., & Sun, Y. (2020). Enhanced photocatalytic activity of GO-TiO<sub>2</sub> composites: The role of GO in the nanocomposite. *Applied Catalysis B: Environmental*, 260, 118195. <https://doi.org/10.1016/j.apcatb.2019.118195>
- [10] Chong, M. N., Jin, B., Chow, C. W. K., & Saint, C. (2010). Recent developments in photocatalytic water treatment technology: A review. *Water Research*, 44(10), 2997-3027.
- [11] Zafar, M., Imran, S. M., Iqbal, I., Azeem, M., Chaudhary, S., Ahmad, S., & Kim, W. Y. (2024). Graphene-based polymer nanocomposites for energy applications: Recent advancements and future prospects. *Results in Physics*, 107655.
- [12] Wu, X. (2021). Applications of titanium dioxide materials. *Titanium Dioxide-Advances and Applications*.
- [13] Vinodhkumar, G., Wilson, J., Inbanathan, S. S. R., Potheher, I. V., Ashokkumar, M., & Peter, A. C. (2020). Solvothermal synthesis of magnetically separable reduced graphene oxide/Fe<sub>3</sub>O<sub>4</sub> hybrid nanocomposites with enhanced photocatalytic properties. *Physica B: Condensed Matter*, 580, 411752.
- [14] Magesan, P., Ganesan, P., & Umapathy, M. J. (2016). Ultrasonic-assisted synthesis of doped TiO<sub>2</sub> nanocomposites: characterization and evaluation of photocatalytic and antimicrobial activity. *Optik*, 127(13), 5171-5180.
- [15] Fattahi, A., Liang, R., Kaur, A., Schneider, O., Arlos, M. J., Peng, P., ... & Zhou, N. (2019). Photocatalytic degradation using TiO<sub>2</sub>-graphene nanocomposite under UV-LED illumination: Optimization using response surface methodology. *Journal of Environmental Chemical Engineering*, 7(5), 103366.
- [16] Deshmukh, S. P., Kale, D. P., Kar, S., Shirsath, S. R., Bhanvase, B. A., Saharan, V. K., & Sonawane, S. H. (2020). Ultrasound assisted preparation of rGO/TiO<sub>2</sub> nanocomposite for effective photocatalytic degradation of methylene blue under sunlight. *Nano-Structures & Nano-Objects*, 21, 100407.
- [17] Eda, G., & Chhowalla, M. (2009). Graphene-based composite thin films for electronics. *Nano Letters*, 9(2), 814-818.
- [18] Nine, M. J., Cole, M. A., Johnson, L., Tran, D. N., & Losic, D. (2015). Robust superhydrophobic graphene-based composite coatings with self-cleaning and corrosion barrier properties. *ACS applied materials & interfaces*, 7(51), 28482-28493.
- [19] Kumaran, V., Sudhagar, P., Konga, A. K., & Ponniah, G. (2020). Photocatalytic degradation of synthetic organic reactive dye wastewater using GO-TiO<sub>2</sub> nanocomposite. *Polish Journal of Environmental Studies*, 29(2), 1683-1690.
- [20] Liang, J., Zhao, Y., Guo, L., & Li, L. (2012). Flexible free-standing graphene/SnO<sub>2</sub> nanocomposites paper for Li-ion battery. *ACS applied materials & interfaces*, 4(11), 5742-5748.
- [21] Liang, Y., Wang, H., Sanchez Casalongue, H., Chen, Z., & Dai, H. (2010). TiO<sub>2</sub> nanocrystals grown on graphene as advanced photocatalytic hybrid materials. *Nano Research*, 3, 701-705.
- [22] Atalay Gengeç, N. (2021). The Effect of Graphene Oxide Exfoliation Degree on Graphene Film Properties. *Bilecik Şeyh Edebali Üniversitesi Fen Bilimleri Dergisi*, 8(1), 345-355.
- [23] Ribao, P., Rivero, M. J., & Ortiz, I. (2017). TiO<sub>2</sub> structures doped with noble metals and/or graphene oxide to improve the photocatalytic degradation of dichloroacetic acid. *Environmental Science and Pollution Research*, 24, 12628-12637.
- [24] Raja, R., Govindaraj, M., Antony, M. D., Krishnan, K., Velusamy, E., Sambandam, A., ... & Rayar, V. W. (2017). Effect of TiO<sub>2</sub>/reduced graphene oxide composite thin film as a blocking layer on the efficiency of dye-sensitized solar cells. *Journal of Solid State Electrochemistry*, 21, 891-903.
- [25] Joshi, N. C., Congthak, R., & Gururani, P. (2020). Synthesis, adsorptive performances and photo-catalytic activity of graphene oxide/TiO<sub>2</sub> (GO/TiO<sub>2</sub>) nanocomposite-based adsorbent. *Nanotechnology for Environmental Engineering*, 5, 1-13.
- [26] He, R., & He, W. (2016). Ultrasonic assisted synthesis of TiO<sub>2</sub>-reduced graphene oxide nanocomposites with superior photovoltaic and photocatalytic activities. *Ceramics International*, 42(5), 5766-5771.
- [27] Timoumi, A., Alamri, S. N., & Alamri, H. (2018). The development of TiO<sub>2</sub>-graphene oxide nano composite thin films for solar cells. *Results in physics*, 11, 46-51.
- [28] Akhair, S. M., Harun, Z., Jamalludin, M. R., Shuhor, M. F., Kamarudin, N. H., Yunos, M. Z., ... & Azhar, M. F. H. (2017). Effect of graphene oxide with controlled stirring time. *Chemical Engineering Transactions*, 56, 709-714.
- [29] Rommozzi, E., Zannotti, M., Giovannetti, R., D'Amato, C. A., Ferraro, S., Minicucci, M., ... & Di Cicco, A. (2018). Reduced graphene oxide/TiO<sub>2</sub> nanocomposite: from synthesis to characterization for efficient visible light photocatalytic applications. *Catalysts*, 8(12), 598.
- [30] Bera, M., Gupta, P., & Maji, P. K. (2018). Facile one-pot synthesis of graphene oxide by sonication assisted mechanochemical approach and its surface chemistry. *Journal of nanoscience and nanotechnology*, 18(2), 902-912.
- [31] Dai, J. F., Wang, G. J., Ma, L., & Wu, C. K. (2015). Surface properties of graphene: relationship to graphene-polymer composites. *Rev. Adv. Mater. Sci*, 40(1), 60-71.
- [32] Scidà, A., Haque, S., Treossi, E., Robinson, A., Smerzi, S., Ravesi, S., ... & Palermo, V. (2018). Application of graphene-based flexible antennas in consumer electronic devices. *Materials Today*, 21(3), 223-230.

## BIOGRAPHIES

**PhD. Candidate (Doctorand) İbrahim Fırat Balkaya** obtained "Casting/Foundry Education Bachelor (2006) & M.Sc. (2014) degrees from Gazi University, Mechanical Engineering Bachelor degree (2018) from Bolu Abant İzzet Baysal University and studies PhD. in Mechanical Engineering Department at Bilecik Şeyh Edebali University Institute of Graduate respectively. He has gained six years of experience in the manufacturing sector. In addition, he also provides custom machine design and production services as a mechanical design engineer. During his doctoral studies, he also worked as a TÜBİTAK researcher for two years, where he was involved in a research project.

**Prof. Dr. Harun Mindivan** completed his Doctorate (Ph.D.) in Materials Science at Istanbul Technical University, Institute of Science and Technology, Turkey, from 2001 to 2007. Prior to that, he earned a Master's degree in Materials Science with a thesis from Istanbul Technical University, Institute of Science and Technology, Turkey, between 1998 and 2001. He also hold a Bachelor's degree in Mechanical Engineering from Atatürk University, Faculty of Engineering, Turkey, which I completed from 1993 to 1997. His research areas include Mechanical Engineering, Metallurgy and Materials Engineering, and Engineering and Technology. He is a faculty member in the Department of Mechanical Engineering at the Faculty of Engineering, Bilecik Şeyh Edebali University, has held several significant administrative positions. From 2014 to 2017, he served as the Director of the Central Research Laboratory at Bilecik Şeyh Edebali University. Between 2016 and 2018, he was the Director of Osmaniye Vocational School, followed by a term as Vice Rector from 2018 to 2019. He also coordinated the Technology Transfer Office (TTO) from 2017 to 2022 and was a Board Member of Anadolu Technology Research Park (ATAP) A.Ş. from 2021 to 2022. In addition to these roles, Prof. Dr. Mindivan was a member of the Public-University-Industry Collaboration (KÜSİ) Working Group established in 2014 by the Ministry of Industry and Technology. He served as the KÜSİ representative for Bilecik province from 2016 to 2020. Throughout his career,

he has been actively involved in numerous TÜBİTAK-TEYDEB and KOSGEB R&D Innovation projects as a referee, observer, and consultant. As a certified R&D Innovation mentor, he also supports companies in evaluating and enhancing their R&D Innovation capacities.

**Asst. Prof. Dr. Nevin Atalay Gengeç** completed her Postdoctoral Research at the University of Northumbria at Newcastle, Faculty of Engineering, Department of Mathematics, Physics, and Electrical Engineering in England from 2019 to 2020. Prior to that, she conducted postdoctoral research at Kocaeli University, Ali Rıza Veziroğlu Vocational School, Department of Environmental Protection Technologies in Turkey, between 2015 and 2017. I earned her Doctor of Philosophy (Ph.D.) in Chemical Engineering from Gebze Technical University, Faculty of Engineering, Department of Chemical Engineering, Turkey, where she studied from 2006 to 2014. Her postgraduate studies were completed at Kocaeli University, Faculty of Science and Letters, Department of Chemistry, where she obtained a Master of Science (M.Sc.) degree in Chemistry from 2002 to 2004. She also hold a Bachelor of Science (B.Sc.) degree in Chemistry from the same institution, which she earned between 1997 and 2002. Her research interests span various fields, including Environmental Technology, Waste Water Collection and Treatment, Chemical Engineering and Technology, Polymer Technology, Environmental Chemistry and Technology, Membrane Technology, Chemistry, Physical Chemistry, Interface Chemistry, Electrochemistry, Functional Polymers, Conductive Polymers, nanocomposites, Characterization of Polymers, Polymeric Films, Polymeric Materials, Surface Chemistry, Engineering and Technology.